Convective transfer from a transverse fin array exposed to two-dimensional turbulent flow

A. T. R. Tindall* and E. A. Vallis†

An experimental investigation of convective transport at the surfaces of a plane transverse fin array exposed to steady turbulent flow was carried out. An electrolytic mass transfer technique was employed in which local and average values of mass transfer coefficients were deduced from the rate of reduction of ferrocyanide ions at the cathode of a diffusion-controlled electrolytic cell. This method has already found wide application in the determination of wall fluxes in high Schmidt number flows and is particularly attractive because of the ease with which results of adequate precision may be obtained. Corresponding heat transfer coefficients were derived from the measured mass transfer coefficients by use of the Chilton–Colburn analogy. The distributions of deduced heat transfer coefficients over the fin and base surfaces of the fin array were studied in areas of developing cavity flow, for Reynolds numbers in the range $1.8\times10^4 \leqslant Re \leqslant 7.2\times10^4$. The values of heat transfer coefficient obtained add to the sparse amount of data presently available for the flow geometry considered.

Keywords: *convection, transverse fins, turbulent flow*

Introduction

In this paper an experimental study of convective mass transfer from a plane transverse fin array is described. The main objective of the work was to investigate the distributions of local convective coefficients over the surfaces of the array in order to provide representative boundary conditions for finite element models of conduction heat transfer through fin arrays, and a reliable data set for the validation of computer models of turbulent recirculating flows.

In order to model effectively the convective heat transfer rates in this flow configuration, it is necessary that the technique employed be applicable where flow separation and impingement occur. Mass transfer analogies have already found wide application to boundary layer flows and have also been used for modelling heat fluxes in more complex regimes.

The rigorous application of analogies of heat and mass transfer requires detailed knowledge of the velocity field and of the structure of turbulence adjacent to the transfer surface. In complex flows in which impingement and recirculation occur, however, this information is not available and it becomes necessary to make recourse to purely empirical relations between heat and mass transfer, such as the Chilton–Colburn analogy. Whilst this was originally derived for a fully developed turbulent flow, it has in recent years been applied with considerable success to more complex situations including developing flow and separation, such as occur in flow normal to heat exchanger tubes[1], the recirculation flow downstream of a sudden expansion[2] and in the normal impingement of an axisymmetric jet onto a plane normal surface[3]. Further support for its use is to be found in the theoretical investigations of near wall flows by Fletcher *et al*[4]. In the present work, the application of the Chilton–Colburn analogy to the flow over plane transverse fins, in which both impingement and recirculation occur, is investigated.

The flow field in the inter-fin cavity may be conveniently subdivided into three areas of interest, namely: the upstream-facing fin surface, the base, and the downstream-facing surface, as shown in Fig 1. Flow recirculates within the fin cavity and fluid from the mainstream flow impinges upon the upstream-facing surface, near the fin tip. Among the earlier studies of heat transfer from plane transverse fins[5–11] some diversity exists in the limited amount of empirical data which has been generated, and whilst it is shown that the results of the present work are in general agreement with those of earlier investigators, careful comparison shows significant differences in detail.

Experimental apparatus

The flow circuit

A schematic diagram of the flow circuit employed is shown in Fig 2. Electrolyte was circulated by a 15 kW stainless steel pump which produced a maximum flow rate of 40 litre/s through the working section. Flow rates

*School of Mechanical and Production Engineering, Leicester Polytechnic, Leicester, LE19 9BH, UK
† Mechanical and Production Engineering Department, Sheffield City Polytechnic, Pond Street, Sheffield S1 1WB, UK
Received 23 May 1985 and accepted for publication in final form on 10 February 1986

were measured using a Nixon Instruments HM80 turbine flowmeter, the calibration of which was checked *in situ* using a weighing tank.

Electrolyte entered the working section through a two-dimensional contraction with an area reduction ratio of 6.67:1. Its profile of matched cubic arcs was based on the recommendations of Morel[12]. Approach to the contraction was through a 4 m length of 500 m × 400 m rectangular ducting, in the upstream end of which was located a PVC flow straightener. This geometry produced a flat velocity profile with low levels of turbulence at the exit from the contraction.

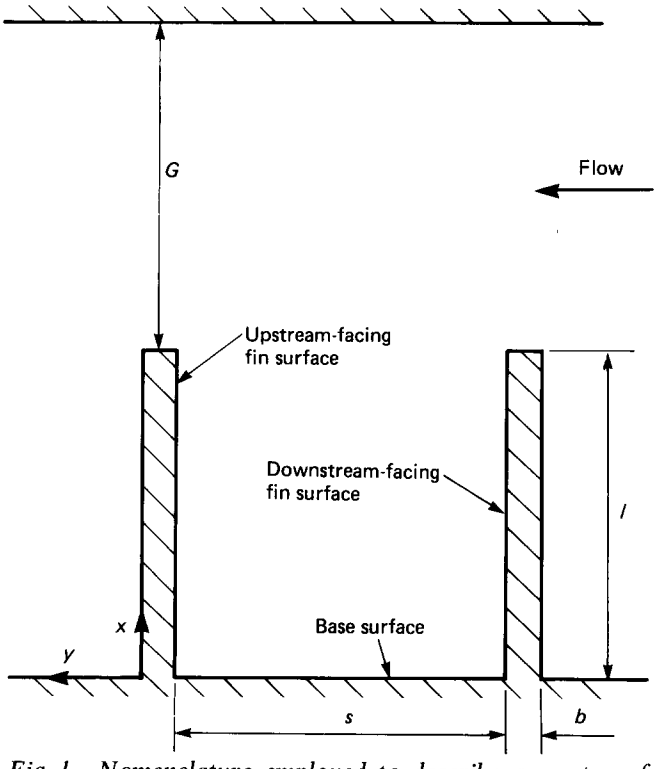

Fig 1 Nomenclature employed to describe geometry of experimental setup

A simple water-cooled heat exchanger was installed upstream of the pump to stabilize the temperature of the electrolyte, which was monitored using a Ni–Cr thermocouple.

Oxidation of the potassium ferricyanide in the electrolyte was prevented by saturating the solution with nitrogen and maintaining a nitrogen atmosphere in the reservoirs. Because of the photosensitivity of potassium ferricyanide the Perspex working section was covered with a black polythene sheet.

The working section

The test section contained a bank of 14 transverse fins, each 500 mm wide, 60 mm long and 6 mm thick. The fins were spaced 60 mm apart and the free channel height between the fin tips and the working section roof was 60 mm. The surfaces of two of the 14 fin-base assemblies were made from nickel and were employed for measuring wall fluxes.

In one of these assemblies, 1.02 mm diameter isolated nickel electrodes were distributed over the base and fin surfaces, with a pitch of 3 mm about the centreline, to measure local values of wall mass fluxes. In the other nickel-surfaced cavity, 10 mm wide isolated nickel strips were mounted on the base and on each fin surface which

Notation

A Surface area of electrode
b Fin thickness
C Concentration
C_b Ion bulk concentration
D Diffusivity
d Diameter of electrode
F Faraday's constant
G Free channel height
I Limiting current
j_H j-factor heat, $NuRe^{-1}Pr^{-1/3}$
j_M j-factor mass, $ShRe^{-1}Sc^{-1/3}$
k Thermal conductivity of fin
L Characteristic length
l Fin height
n Valency change in reaction
Nu Nusselt number, $\alpha L/k$
Nu_B Mean Nusselt number for base surface, $\bar{\alpha}G/k$
Nu_{BP} Maximum local Nusselt number for base surface, $\alpha G/k$
Nu_D Mean Nusselt number for downstream-facing fin surface, $\bar{\alpha}G/k$
Nu_{DP} Maximum local Nusselt number for downstream-facing surface, $\alpha G/k$
Nu_M Mean Nusselt number for upstream- and downstream-facing fin surfaces, $\bar{\alpha}_F G/k$
Nu_U Mean Nusselt number for upstream-facing fin surface, $\bar{\alpha}G/k$
Nu_{UP} Maximum local Nusselt number for upstream-facing fin surface, $\alpha G/k$
Pr Prandtl number
Re Reynolds number, VGv^{-1}
Sc Schmidt number, vD^{-1}
Sh Sherwood number, βGD^{-1}
s Inter-fin spacing
t Time
u_{ion} Mobility of ions
V Mean velocity of flow in main stream
x,y Cartesian coordinates
α Heat transfer coefficient
$\bar{\alpha}$ Average heat transfer coefficient over surface considered
$\bar{\alpha}_B$ Average heat transfer coefficient over base surface
$\bar{\alpha}_F$ Average heat transfer coefficient over upstream- and downstream-facing fin surfaces
β Mass transfer coefficient
β_B Average mass transfer coefficient over cavity base surface
β_D Average mass transfer coefficient over downstream-facing surface
β_F Average mass transfer coefficient over upstream- and downstream-facing fin surfaces
β_U Average mass transfer coefficient over upstream-facing surface
δ Sum of heights of upstream- and downstream-facing fin surfaces in cavity under consideration
v Kinematic viscosity
ϕ Potential

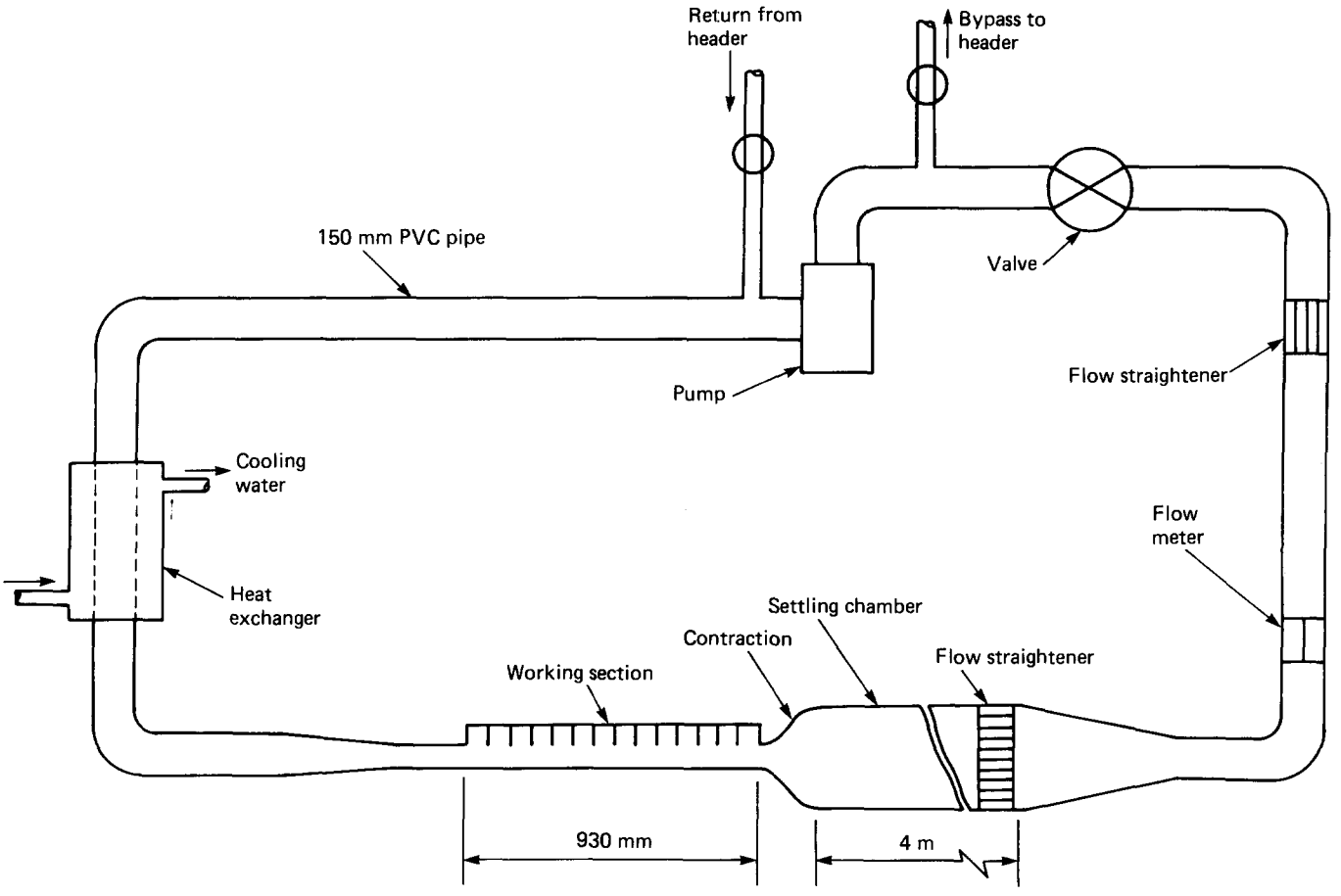

Fig 2 Schematic diagram of flow circuit

bounded the cavity. These strips extended in the direction of flow for the full length of the surfaces, and were used to determine the total mass transfer rate to the surfaces in order to obtain the average value of the mass transfer coefficient for each surface. These instrumented cavities could be moved to any desired position in the array.

A 1000 mm × 500 mm nickel anode was located flush on the floor of the test section.

Electrolyte

1400 litres of electrolyte with the following composition were prepared:

0.005 M potassium ferricyanide (K_3 Fe $(CN)_6$)
0.005 M potassium ferrocyanide (K_4 Fe $(CN)_6$)
2.07 M sodium hydroxide (NaOH)

Analytical grade (ANALAR) chemicals were used throughout, the solution being made up with de-ionized water. The transport properties for the electrolyte were determined from the empirical data of Bazan and Arvia[13] and Eisenberg *et al*[14]. The Schmidt number of the electrolyte was 3300.

Electrical circuits

The electrical circuit used to measure the rate of diffusion of ferricyanide ions to the cathodes of the cell is shown in Fig 3. The currents were measured using a current-to-voltage converter online to a Commodore 2001 microcomputer. This computer was used to control

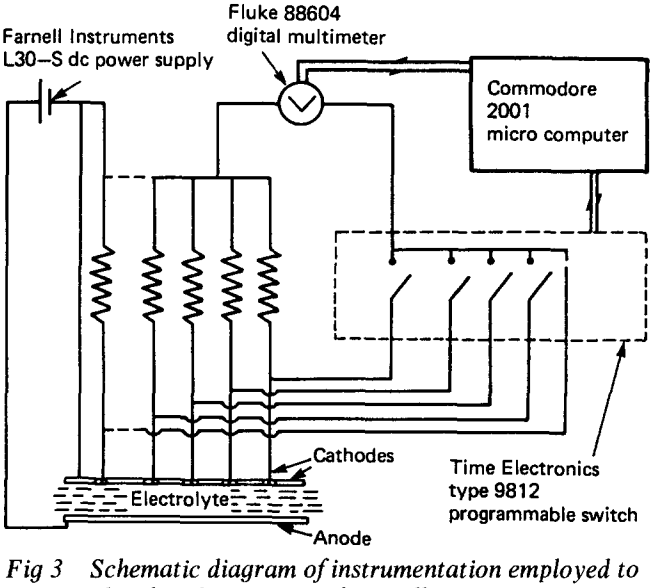

Fig 3 Schematic diagram of instrumentation employed to measure local and mean transfer coefficients

electrode selection and sampling time, in addition to data processing.

Experimental procedure

During initial trials, good limiting current plateaus were obtained (Fig 4) and during the tests the cell potential was maintained at 0.9 V.

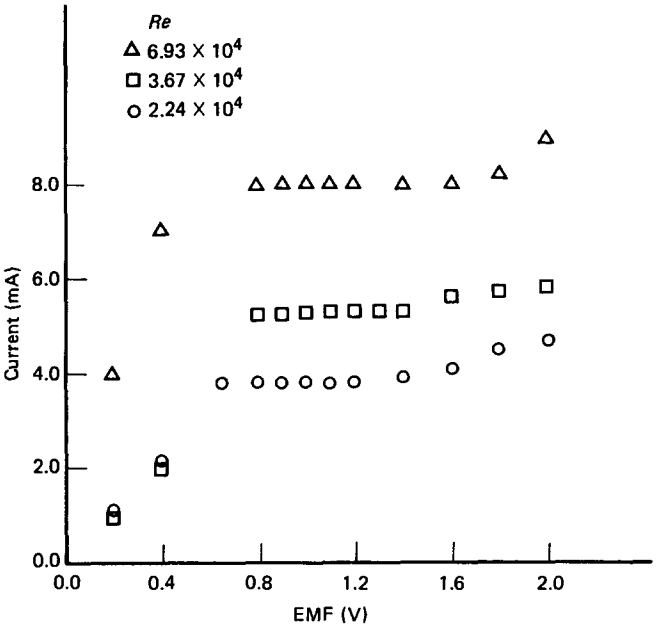

Fig 4 Typical limiting current curves

Values of local and mean mass transfer coefficients were measured on the surfaces of the instrumented fin and base assemblies mounted in positions 1 to 9 for $1.8 \times 10^4 \leqslant Re \leqslant 7.2 \times 10^4$.

At the end of the electrochemical tests the electrolyte in the flow circuit was replaced by water and, using neutral buoyancy polystyrene beads of 1.5 mm diameter as tracer particles, still and video films were made of the flows in the inter-fin cavities investigated in the electrochemical tests.

Data processing

The rate of discharge for a certain species of ion may be expressed as

$$\frac{I}{(nFA)} = -D\frac{\partial C}{\partial y} - Cu_{\text{ion}}\frac{\partial \phi}{\partial y} \tag{1}$$

For the case when ionic migration is negligible and the cell is diffusion controlled, Eq (1) becomes:

$$\frac{I}{nFA} = \beta C \tag{2}$$

From this expression, the mass transfer coefficient may be readily obtained. Since the primary purpose of the experimental work was to provide data for heat transfer calculations, the mass transfer coefficients determined in the present work were transformed to equivalent heat transfer coefficients using the Chilton–Colburn analogy[15]:

$$j_M = \frac{Sh}{ReSc^{1/3}} = j_H = \frac{Nu}{RePr^{1/3}} \tag{3}$$

Results and discussion

Flow in each of the cavities of the fin geometry under investigation was characterized by the presence of a large flat-sided eddy, the centre of which was displaced downstream of the centre of the cavity (see Fig 5). This is in agreement with the results of earlier workers, eg Stynes and Myers[6] and Ueda and Harada[7].

A stagnation point, close to the tip of each upstream-facing fin surface was also identified in the present work, whilst Wieghardt[16] and Stynes and Myers[6] also detected the presence of small eddies, in each of the two root corners of the fin cavities. No measurements of eddy intensity were made but a numerical model of the flow[17], developed in conjunction with the present empirical work, shows a gradual decrease in eddy intensity in the cavities as the flow proceeds downstream and the boundary layer above them increases in thickness. The shapes of the streamlines predicted by the model appear, as was found in the flow visualization studies, to be substantially the same in all cavities.

Mean heat transfer coefficient

The results for mean convective heat transfer coefficients obtained from mass transfer measurements on the isolated strip electrodes are shown in Figs 6 and 7. From these results it can be seen that there is no significant variation in mean convective heat transfer coefficient with distance from the entrance to the fin array for the configuration considered.

Using the Chilton–Colburn analogy, the following data correlations for the average values of Nusselt number over the surfaces of the cavity were derived.

For the upstream facing surface:

$$Nu_U = 0.14Re^{0.66}$$

For the downstream facing surface:

$$Nu_D = 0.11Re^{0.65}$$

For the base surface:

$$Nu_B = 0.33Re^{0.56}$$

From Fig 8 it can be seen that the present results fall between the experimental values of Roizen *et al*[8] and

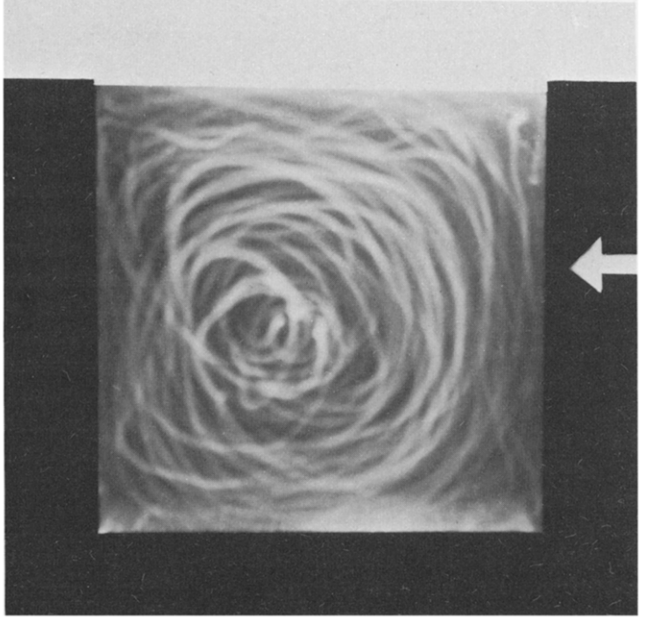

Fig 5 Typical cavity flow: Cavity 8, $Re = 5 \times 10^4$, scale 1:1

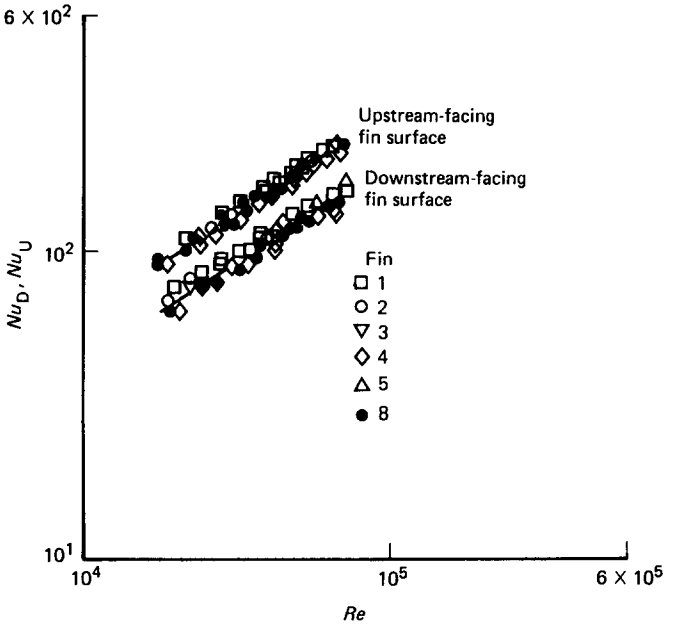

Fig 6 Correlation of data obtained from strip electrodes on fin surfaces

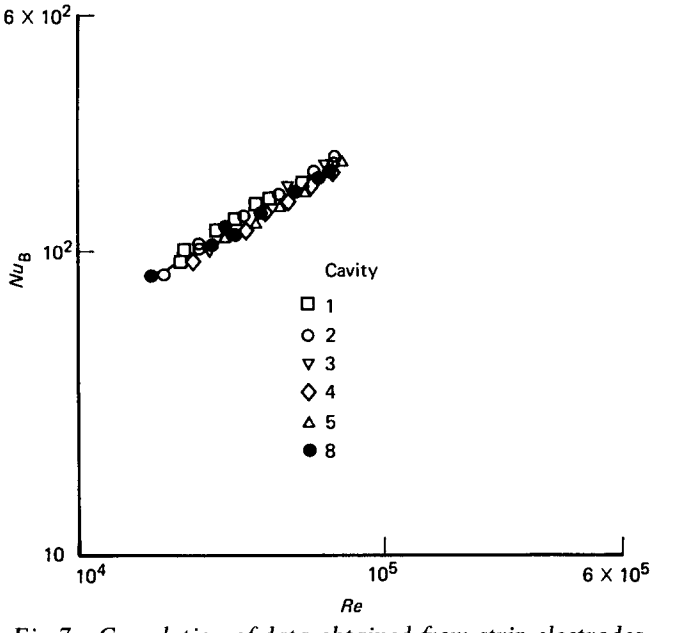

Fig 7 Correlation of data obtained from strip electrodes on cavity base

Okamoto and Kameoka[9]. These earlier investigators attribute a value of 0.8 to the exponent of the Reynolds number, some 30% higher than that of the current work. However, support for the present results may be found in the experimental investigations of heat transfer in the recirculation zone downstream of axisymmetric sudden expansions by Tagg *et al*[2] and Krall and Sparrow[18]. Further support for a Reynolds number exponent less than 0.8 in areas of recirculation is also to be found in the review of heat and mass transfer by Launder[19] and in the theoretical analysis of heat transfer in separated flows by Spalding[20].

Local mass transfer coefficient

For all the inter-fin cavities investigated, the form of the distribution of local mass transfer coefficient over the upstream-facing fin and inter-fin base surfaces were found to be independent of *Re*. This was also found to be so on the downstream-facing fin surfaces for $y/l < 0.65$, but for values of $y/l > 0.65$ the distributions of local mass transfer coefficient were found to assume two distinctly different forms for values of *Re* above and below 4×10^4.

The distributions of local mass transfer coefficient over the fin and base surfaces were found to be independent of the distance of the fin cavity from the entrance to the array except for the first cavity, where the wall fluxes were found to be measurably higher due to the influence of the thin shear layer at exit from the slot nozzle.

The distribution of local values of mass transfer

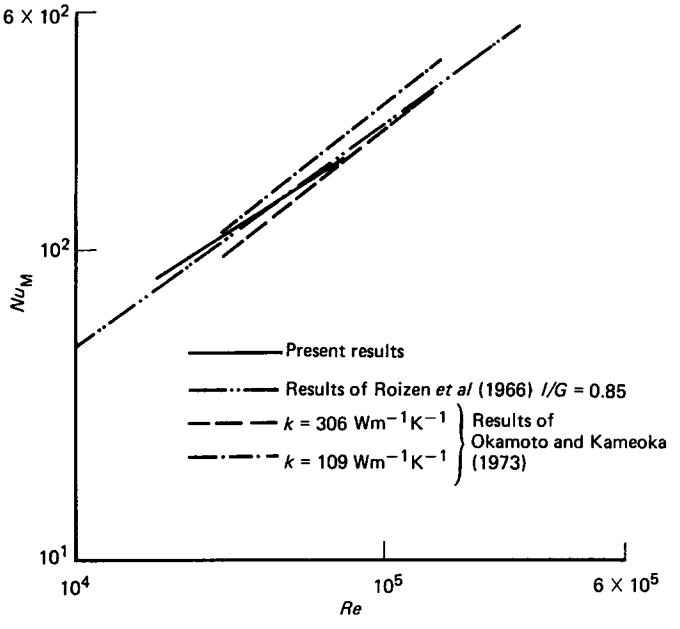

Fig 8 Comparison of present results with those of Roizen et al[8] *and Okamoto and Kameoka*[9]

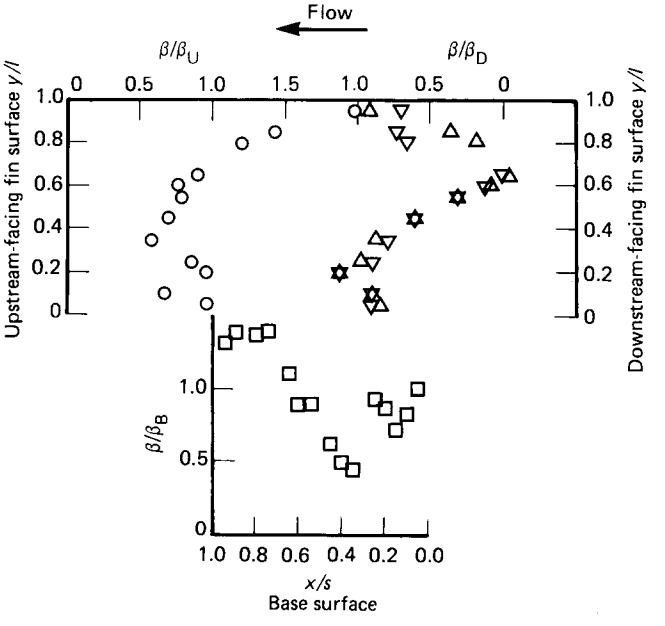

Fig 9 Distribution of local mass transfer coefficient over cavity surfaces

coefficient, obtained by averaging values recorded at corresponding positions in all cavities, is shown in Fig 9. The highest value of mass transfer coefficient corresponds to the impingement zone created by attachment of the main stream flow, near the tip of the upstream-facing surface. Major peak values of mass transfer occurred on the base and downstream-facing fin surfaces where the flow reattaches downstream of the small eddies in the root corners; other secondary peaks, caused by the presence of small eddies, occur near the tip of the downstream-facing surface and in the root corners of the cavity.

Few directly comparable experimental data for local heat transfer coefficients exist for the flow conditions and geometry currently under consideration. The results from Refs 8 and 9, illustrated in Fig 10, differ significantly from each other, but those of Roizen *et al*[8] are in reasonable agreement with the present results. However, due to the low resolution of the technique adopted by Roizen *et al* in which each strip heater occupied approximately 19% of the area of the surface under investigation, their observed variation of local heat transfer coefficient along each surface was somewhat less than that found in the present work.

The locations of the major and secondary peaks on the surfaces of the cavities are shown in Table 1.

Data correlations were derived for the major peak values of Nusselt number on the inter-fin cavity surfaces as follows.

Upstream facing surface:

$$Nu_{UP} = 0.83 Re^{0.56}$$

Downstream facing surface:

$$Nu_{DP} = 0.14 Re^{0.67}$$

Base surface:

$$Nu_{BP} = 0.14 Re^{0.67}$$

These are illustrated in Fig 11.

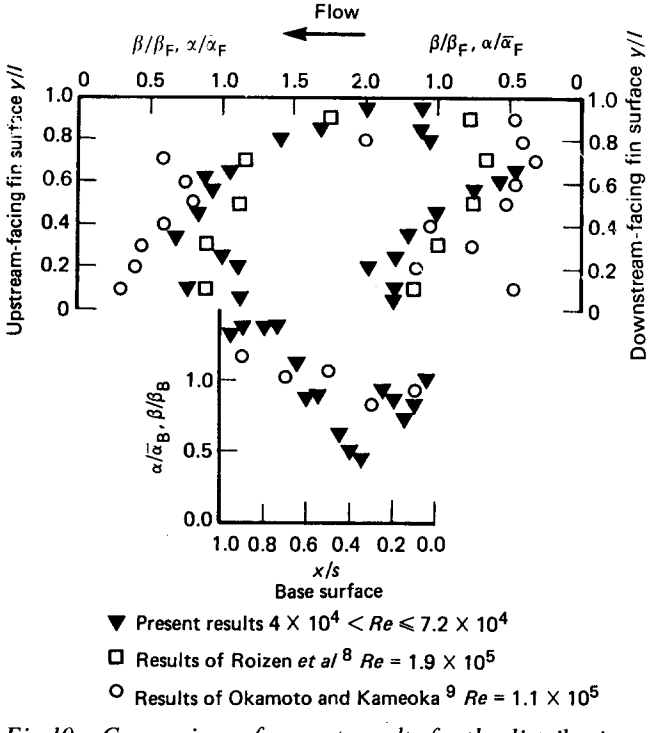

Fig 10 Comparison of present results for the distributions of local convective coefficients with those of Roizen et al[8] *and Okamoto and Kameoka*[9]

Table 1 Location of major and secondary peak values of Nusselt number for $1.8\times10^4 \geqslant Re \geqslant 7.2\times10^4$

	Location of peak values of Nusselt number	
Surface	Major	Secondary
Upstream-facing	$y//>0.95$	$y//=0.2$
Downstream-facing	$y//=0.2$	$y//=0.85$ ($Re<4\times10^4$) $y//=0.95$ ($Re>4\times10^4$)
Base	$x/s=0.85$	$y//=0.25$

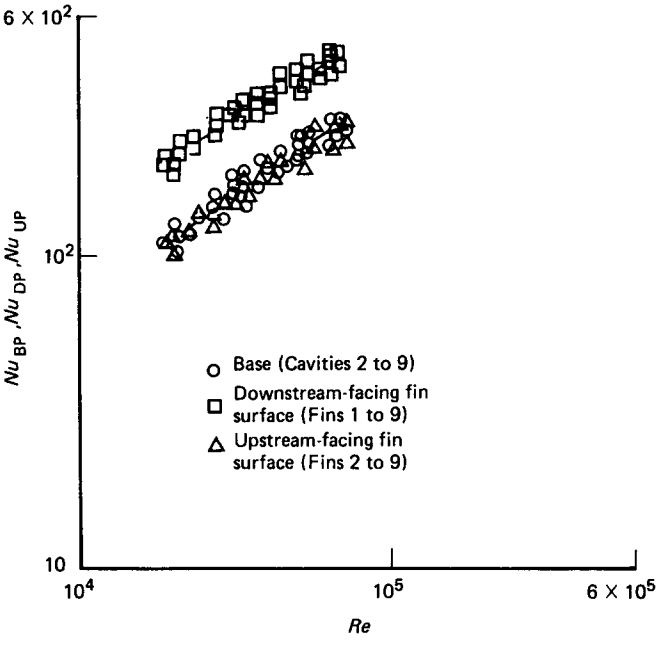

Fig 11 Correlation of data for maximum value of Nusselt number on the upstream-facing fin, base and downstream-facing fin surfaces

Conclusions

Peak values of heat transfer coefficient have been observed on all surfaces of the transverse fin array considered, with particularly high values occurring due to the impingement of the main stream flow on the upstream-facing fin surface. For the downstream-facing and base surfaces the differences between the maximum and mean values of heat transfer coefficient are in excess of 25%, whilst for the upstream-facing fin surface the difference is greater than 45%.

Few data from heat transfer experiments exist for the geometry under consideration, and, in the two earlier investigations cited which allow direct comparisons of average values of Nusselt number to be made, their results differ by more than 20%. The present results fall between those obtained in these earlier studies but a significant discrepancy exists in respect of the Reynolds number dependence of the Nusselt number, for which the present results suggest a Reynolds number exponent of $\frac{2}{3}$, compared with $\frac{4}{5}$ proposed by the earlier workers. The present result, however, finds some support in the investigations of heat fluxes in other separated flows[2,18,19], and would appear to be a more appropriate value for use in design applications than that currently in vogue.

References

1 **Gay B., Mackley N. V. and Jenkins J. D.** Shell-side heat exchanger in baffled cylindrical shell and tube exchangers: an electrochemical mass transfer modelling technique. *Int. J. Heat Mass Transfer, 1976,* **19**, *995–1001*

2 **Tagg D. J., Patrick M. A. and Wragg A. A.** Heat and mass transfer downstream of abrupt nozzle expansions in turbulent flow. *Trans. Inst. Chem. Engrs, 1979,* **57**, *176–181*

3 **Vallis E. A., Patrick M. A. and Wragg A. A.** Radial distribution of convective heat transfer co-efficient between an axi-symmetric turbulent jet and a flat plate held to the flow. *Proc. 6th Int. Conf. on Heat Transfer, Aug 7–11 1978, Toronto, Nat. Res. Council of Canada, Toronto, 1978, Vol 5, 297–303*

4 **Fletcher D. F., Maskell S. J. and Patrick M. A.** Theoretical investigation of the Chilton–Colburn analogy using a modified form of the Van Driest Eddy Viscosity Hypothesis. *Trans. I. Chem. E., 1982,* **60**, *122–129*

5 **Harris M. J. and Wilson J. T.** Heat transfer and fluid flow investigation on large scale transverse fins. *J. Brit. Nuclear Energy Conf., 1961,* **6**, *330–334*

6 **Stynes S. K. and Myers J. E.** Transport from extended surfaces. *A. I. Chem. E. J., 1964,* **10**, *437–444*

7 **Ueda T. and Harada I.** Experiment of heat transfer on the surfaces with transverse fins for flow direction. *Trans. Japan Soc. Mech. Engrs. 1964,* **7**, *559–568*

8 **Roizen L. I., Dulkin I. N. and Rakashina N. I.** Heat transfer in flow over straight transverse fins. *Inzherrerrio-Fizicheskii Zhurral, 1966,* **11**, *148–153*

9 **Okamoto Y. and Kameoka T.** Study on convective heat transfer from planar fin surfaces. *Heat Transfer–Japanese Res., 1973,* **2**, *1–13*

10 **Kameoka T. and Nakamura K.** Investigation on convective heat transfer from transverse finned surfaces. *Trans. Japan Soc. Mech. Engrs., 1975,* **18**, *33–40*

11 **Kameoka T. and Nakamura K.** Investigation on convective heat transfer from finned plate surface. *Heat Transfer–Japanese Res., 1977,* **6**, *41–54*

12 **Morel T.** Design of two-dimensional wind tunnel contractions. *Trans. ASME, J. Fluids Engg, 1976, Paper No 76/WA/FE/4*

13 **Bazan J. C. and Arvia A. J.** The diffusion of ferro-ferricyanide ions in aqueous solutions of sodium hydroxide. *Electrochemica Acta, 1965,* **10**, *1025–1032*

14 **Eisenberg M., Tobias C. W. and Wilkie C. R.** Selected physical properties of ternary electrolytes employed in ionic mass transfer studies. *J. Electrochem. Soc., 1956,* **103**, *413–416*

15 **Chilton T. H. and Colburn A. P.** Mass transfer (absorption) coefficients. *Ind. Eng. Chem., 1934,* **26**, *1183–1187*

16 **Wieghardt K.** Erhohung des turbulenten reihungswiderstandes durch oberfachenstrorungen. *Forschungshafte fur Schiffstechnik, 1953,* **2**, *65–67*

17 **Vallis E. A. and Tindall A. T. R.** Numerical Modelling of Turbulent Flows over Transverse Fin Arrays. *HCHE, Int. Rept., ENG/VT/84/1, 1984*

18 **Krall K. M. and Sparrow E. M.** Turbulent heat transfer in separated re-attached and re-developing region of circular tubes. *ASME J. Heat Transfer, Feb 1966,* **88**(*1*), *131–136*

19 **Launder B. E.** Heat and mass transport. *Topics in Appl. Phys., 1978,* **12**, *279–284*

20 **Spalding D. B.** Heat transfer from turbulent separated flows. *J. Fluid Mech., Jan 1967,* **27**(*1*), *97–109*

BOOK REVIEW

Fluid Mechanics and Transfer Processes

J. M. Kay and R. M. Nedderman

Undergraduate students have difficulty in properly understanding flow processes in engineering. Many texts deal with this by a combination of an explanation of the laws of physics involved in a particular phenomenon and then support it with a simple worked example. This usually serves as a model for the students who can then work through a series of questions at the end of the chapter, so reinforcing the lesson. Fluid Mechanics and Transfer Processes by J. M. Kay and R. M. Nedderman does not include such questions and, therefore, most undergraduate students will not find this an acceptable text book.

The text itself is well written and begins its many sections with a simple description of flow type and a lucid development of the ideas and basic analysis involved. However there is an implicit reliance on students having a comprehensive mathematical ability; the basic analysis is often developed for complicated processes in a limited number of steps. For instance, at the beginning of chapter 3 the development of Bernoulli's equation from the Euler equation is at a sensible pace. However, by the end of chapter 3 when dealing with vorticity and rotational flow too much is assumed of the student. Numerical examples are shown in skeleton form and therefore, place a heavy reliance on the student's ability which may be premature.

For the mathematically inclined who study in a relatively relaxed environment this text offers an excellent route to understanding the subject. It explains the basic mechanisms of fluid, heat and mass flow in a simple and elegant manner and develops the subject logically and quickly to more complex situations. Advanced students, especially those on master's degree courses, who require to revise and develop material by their own study would find this text book most helpful.

Dr P. J. Moss
School of Mechanical, Materials and Civil Engineering, RMCS, Shrivenham, Swindon

Published, price £45 ($69.00) hard cover, £17.50 ($29.95) paperback, by Cambridge University Press. Cambridge University Press, Shaftesbury Road, Cambridge CB2 2RU, UK